Naphthylphthalamic acid associates with and inhibits PIN auxin transporters

Lindy Abas[a,1,2], Martina Kolb[b,1], Johannes Stadlmann[c], Dorina P. Janacek[b], Kristina Lukic[d], Claus Schwechheimer[b], Leonid A. Sazanov[d], Lukas Mach[a], Jiří Friml[d], and Ulrich Z. Hammes[b,2]

[a]Department of Applied Genetics and Cell Biology, University of Natural Resources and Life Sciences (BOKU), 1190 Vienna, Austria; [b]Plant Systems Biology, School of Life Sciences Weihenstephan, Technical University of Munich, 85354 Freising, Germany; [c]Department of Chemistry, University of Natural Resources and Life Sciences (BOKU), 1190 Vienna, Austria; and [d]Institute of Science and Technology Austria, 3400 Klosterneuburg, Austria

Edited by Julian I. Schroeder, University of California at San Diego, La Jolla, CA, and approved November 12, 2020 (received for review October 5, 2020)

***N*-1-naphthylphthalamic acid (NPA) is a key inhibitor of directional (polar) transport of the hormone auxin in plants. For decades, it has been a pivotal tool in elucidating the unique polar auxin transport-based processes underlying plant growth and development. Its exact mode of action has long been sought after and is still being debated, with prevailing mechanistic schemes describing only indirect connections between NPA and the main transporters responsible for directional transport, namely PIN auxin exporters. Here we present data supporting a model in which NPA associates with PINs in a more direct manner than hitherto postulated. We show that NPA inhibits PIN activity in a heterologous oocyte system and that expression of NPA-sensitive PINs in plant, yeast, and oocyte membranes leads to specific saturable NPA binding. We thus propose that PINs are a bona fide NPA target. This offers a straightforward molecular basis for NPA inhibition of PIN-dependent auxin transport and a logical parsimonious explanation for the known physiological effects of NPA on plant growth, as well as an alternative hypothesis to interpret past and future results. We also introduce PIN dimerization and describe an effect of NPA on this, suggesting that NPA binding could be exploited to gain insights into structural aspects of PINs related to their transport mechanism.**

auxin transport | NPA | PIN | auxin transport inhibitor | naphthylphthalamic acid

Many aspects of plant growth are controlled by the hormone auxin. A distinct feature of auxin is that its hormonal action requires it to be actively transported between cells and ultimately throughout the whole plant in a controlled directional or polarized manner, a process known as polar auxin transport (PAT). The ability of plants to perform PAT is ascribed to the auxin export activity of PIN transporters (1). Plasma membrane PINs can be restricted to a specific side of cells (2), and when this polarity is maintained in continuous plant cell files, the combined activity of identically localized PINs results in auxin flowing in that direction (3). This lays the vectorial foundations for PAT to create local auxin gradients and plant-wide PAT streams that are critical for auxin action and normal plant growth (4, 5).

Synthetic PAT inhibitors such as *N*-1-naphthylphthalamic acid (NPA) were initially developed as herbicides and then subsequently exploited by researchers to identify and characterize the unique PAT-based mechanisms that drive plant development (6). Having been used for over six decades, the question as to how NPA actually inhibits PAT has been keenly pursued. Several putative modes of action have been proposed, but the topic remains to date not fully or satisfactorily resolved (6).

Early studies established NPA binding with high affinity to membrane-integral components of plant membranes (7–10). With the later discovery of *pin1* mutants bearing their distinct bare inflorescences reminiscent of NPA-treated plants (11), followed by identification of the PIN gene family and gradual confirmation that PINs were NPA-sensitive auxin transporters that mediated PAT (1–5), it was apparent that the physiological and genetic evidence overwhelmingly linked NPA to inhibition of PIN activity (6). However, direct molecular association of NPA with PINs has never been reported (6). Instead, a substantial body of data has accumulated suggesting that the NPA target is not PIN itself, but rather other proteins or complexes that either actively coparticipate in PAT or are indirectly involved in control of PAT components (6, 12). Members of the B-family of ABC transporters, such as ABCB1 and ABCB19, showed high-affinity NPA binding and NPA-sensitive auxin export (1, 12–15), thus leading to proposals that they may either physically interact with PINs, or functionally interact such that their nonpolar auxin export activity contributes to PAT and/or to regulation of PINs (12, 16). In these scenarios, PIN/PAT would be rendered vulnerable to the NPA sensitivity of ABCB. However, these schemes are not yet fully resolved, are not fully consistent with key genetic and physiological data (6), and are particularly obfuscated by ABCB1/19 functioning both interactively and independently from PINs (1, 12, 15–20), with ABCB-PIN interaction occurring in an as-yet-unclarified manner (15, 18).

A further twist in assigning ABCBs as the main NPA target is their regulation by their chaperone TWD1/FKBP42 (14, 16), with TWD1 itself also being an NPA-binding protein (14, 17). NPA interferes with this regulation and affects TWD1-ABCB interaction, but curiously NPA cannot bind stably to the ABCB-TWD1 complex (14, 17). As TWD1 has also been implicated in NPA-sensitive actin-based PIN trafficking (17), this has led to a model proposing that TWD1 could mediate the NPA

Significance

The plant hormone auxin regulates many aspects of plant life and has the unique ability to flow throughout the plant in defined directions, as observed by Darwin over a century ago. The chemical NPA inhibits this directional flow, thereby severely affecting plant growth. In studying the specific effects of NPA, researchers have also uncovered general principles underlying plant development. Exactly how NPA inhibits directional auxin flow is unclear. NPA interacts with proteins that can transport auxin, such as ABCB transporters, and we show here that NPA also associates with and inhibits the major transporters that specialize in directional auxin flow—PINs. This explanation of NPA action will guide future research and may help reveal how PINs perform auxin transport.

Author contributions: L.A., M.K., C.S., L.M., J.F., and U.Z.H. designed research; L.A., M.K., J.S., and D.P.J. performed research; K.L., L.A.S., and J.F. contributed new reagents/analytic tools; L.A., M.K., J.S., and U.Z.H. analyzed data; and L.A. wrote the paper.

The authors declare no competing interest.

This article is a PNAS Direct Submission.

[1]L.A. and M.K. contributed equally to this work.

[2]To whom correspondence may be addressed. Email: melinda.abas@boku.ac.at or ulrich.hammes@wzw.tum.de.

This article contains supporting information online at https://www.pnas.org/lookup/suppl/doi:10.1073/pnas.2020857118/-/DCSupplemental.

Published December 22, 2020.

sensitivities of both ABCB and PINs, thus presenting TWD1 as a modulator of PAT (17, 21). In an analogous scheme in some plant species, CYPA immunophilins such as tomato DGT, which are functionally similar to TWD1/FKBP42, are suggested to replace TWD1 in modulating auxin transporters and transducing NPA effects to PINs (12, 21).

Similar to TWD1, BIG/TIR3 has also been associated with NPA and PIN trafficking (22). Given the undisputed role of trafficking in controlling PIN polarity (5), these reported effects warrant attention, although they are inconsistent with other reports that NPA perturbs neither vesicular trafficking nor actin dynamics in conditions where auxin transport is inhibited (23, 24). Together with trafficking, phosphorylation is another key modulator of PIN polarity as well as activity (5), so it is not surprising to find hypotheses suggesting that NPA could interfere with critical phosphorylation events (6), particularly as PID, a kinase crucial for PIN trafficking and activation, has also been connected to ABCB function and TWD1/ABCB/NPA interactions (25). Others propose that NPA may mimic natural compounds in their capacity as endogenous regulators of PAT, with plant flavonoids being suspected candidates (6, 26). Since flavonoids can compete with or inhibit ATP-binding in mammalian kinases and ABC transporters (27, 28), and as flavonoids can bind to and inhibit PID (25), a phosphorylation-based NPA mode of action would overlap with this hypothesis and poses the question whether NPA acts similarly as an ATP mimic.

With these many potential NPA-affected pathways, there is a need to distinguish between low- and high-affinity NPA targets and possible secondary effects due to prolonged PAT inhibition. Current consensus is that low concentrations of NPA (<10 μM) cause direct inhibition of auxin transporters in PAT (21) and the consequent physiological effects seen in planta (IC_{50} 0.1 to 10 μM) (7, 9, 19, 23, 29). This is associated with high-affinity binding to membranes (K_d 0.01 to 0.1 μM) (7, 8) and the inhibition of PIN/ABCB activity in short-term auxin transport assays (1, 14, 18, 20, 23). In contrast, NPA is thought to affect trafficking (21, 30) and other non-PAT processes (31) when used at higher doses (50 to 200 μM NPA), presumably via binding to its lower-affinity targets, although excessive NPA exposure may also have fast-acting toxic side effects (23). As the in vitro affinity of TWD1 for NPA is surprisingly low (K_d ~100 μM) (17), the TWD1-mediated NPA effects on PIN/PAT are thought to be of the low-affinity type and linked to trafficking perturbations (17, 21). However, as NPA is always externally applied to plants or cells, it is not clear how or where the drug distributes or accumulates, and thus there may be discrepancies between actual and reported/apparent effective concentrations, as might be the case for TWD1 (17). Finally, NPA also binds with low affinity to inhibit APM1, an aminopeptidase implicated in auxin-related plant growth, but as with trafficking effects, this low-affinity NPA interaction is not connected to direct regulation of PAT (31).

Thus, the available data proffer various indirect mechanisms that could lead to NPA inhibition of PIN-mediated PAT, but the proposed schemes have complicating aspects and struggle at times to satisfactorily explain the prime effects of NPA. Here we propose an alternative simpler scenario involving a more direct link between NPA and PINs that would resolve some of these currently outstanding issues. We present evidence from heterologous transport assays, classical in situ membrane binding, and oligomerization studies which collectively suggest that NPA can interact directly in a high-affinity manner with PINs, leading to conformational or structural effects and inhibition of auxin export activity.

Results and Discussion

NPA Inhibits PIN-Mediated Auxin Transport in Oocytes. A notable advancement in auxin transport research was the recent establishment of a *Xenopus* oocyte assay to measure export activity of *Arabidopsis thaliana* PINs (32). As with previous assays, it monitors the retention of radiolabeled ^{3}H-indoleacetic acid (IAA). However, the ability to inject ^{3}H-IAA as well as any inhibitory drugs directly into oocytes avoids the vagaries associated with external application and passive preloading of both in previous heterologous assays. More importantly, there is also a unique on/off activity switch for the expressed *At*PINs by virtue of the absence or presence of coexpressed mandatory activating kinases (32). We thus utilized this improved and tractable system to investigate NPA effects on PIN activity.

When coinjected with ^{3}H-IAA into oocytes (NPA_{in}), 10 μM NPA (final internal concentration) abolished ^{3}H-IAA export mediated by kinase-activated *At*PIN1 or *At*PIN3, whereas 1 μM NPA_{in} caused partial inhibition (Fig. 1 *A* and *C*). We also saw NPA_{in} inhibition of *At*PIN6 export activity (*SI Appendix*, Fig. S1*A*), confirming that this noncanonical PIN is NPA-sensitive (33). NPA_{in} inhibition of PIN-dependent ^{3}H-IAA export occurred with either PID or D6PK as the activating kinase (Fig. 1*C*); thus kinase identity was not crucial.

We checked that inhibition of PIN activity was not due to deleterious effects of NPA on general oocyte viability by measuring ^{3}H-IAA or ^{14}C-leucine import by *At*AUX1 and *At*CAT6, respectively. In contrast to PINs, the activity of these other plasma membrane transporters was not compromised by 10 μM NPA_{in} (*SI Appendix*, Fig. S1 *C* and *D*), showing that NPA inhibits neither global transport nor ^{3}H-IAA transport in general. We found no effect of NPA_{in} on ^{3}H-IAA retention in control oocytes expressing inactive PIN without kinase, expressing kinase only, or neither (Fig. 1*C* and *SI Appendix*, Fig. S1 *A* and *E*), confirming that NPA

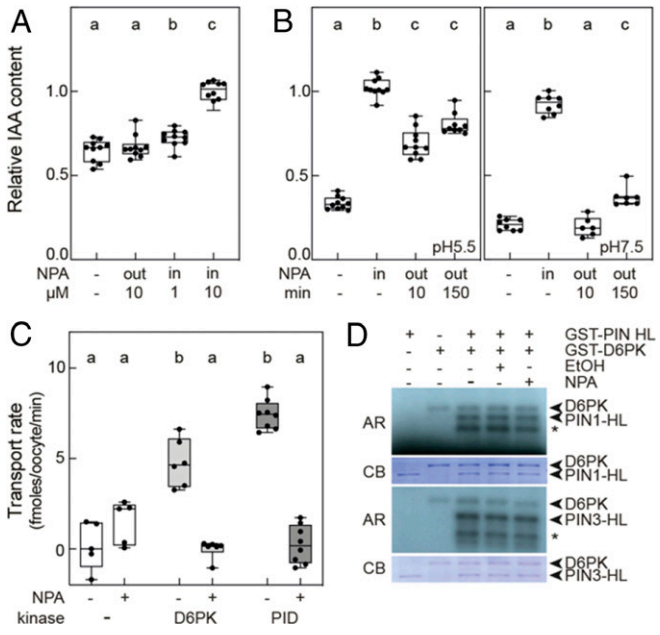

Fig. 1. NPA inhibits PIN-mediated ^{3}H-IAA efflux in oocytes. (*A*) In oocytes, coinjected NPA_{in} fully (10 μM) or partially (1 μM) inhibits ^{3}H-IAA efflux mediated by PIN1 (+YFP:D6PK), whereas external 10 μM NPA_{out} added immediately to the pH-7.5 medium has no effect (ANOVA; $n = 12$; a–c, b–c, $P < 0.001$; a–b, $P = 0.029$). (*B*) In pH-5.5 medium (*Left*), external 10 μM NPA_{out} is effective at inhibiting ^{3}H-IAA efflux mediated by PIN3 (+YFP:D6PK) after a 10-min preincubation whereas external NPA_{out} at pH 7.5 (*Right*) causes only partial inhibition after 2.5 h, compared to full inhibition by coinjected 10 μM NPA_{in} (ANOVA; $n = 10$; $P < 0.0001$ for all subsets). (*C*) Coinjected 10 μM NPA_{in} fully inhibits PIN3-mediated ^{3}H-IAA efflux from oocytes independent of the choice of activating kinase, YFP:D6PK or PID (two-way ANOVA, $n = 5$ to 8; $P < 0.001$ for ±kinase as well as ±NPA subsets). (*D*) In [γ-^{32}P]-*ATP* in vitro kinase assays, 10 μM NPA does not inhibit D6PK autophosphorylation or D6PK phosphorylation of PIN1 (*Upper*) or PIN3 (*Lower*) hydrophilic loops (HL); A single asterisk indicates PIN degradation products. AR, autoradiogram; CB, Coomassie Blue gel.

only affected outward movement of ^{3}H-IAA when mediated by active PINs. As a further control, we ruled out NPA being a direct competitor of IAA transport by performing transport assays with ^{3}H-NPA. We found that ^{3}H-NPA was not transported by PIN1 or PIN3 (with YFP:D6PK) in oocytes (*SI Appendix*, Fig. S1*B*), complementing earlier in planta data that NPA is not polarly transported in maize (7). Collectively, these controls indicate that the effect of NPA on ^{3}H-IAA retention in oocytes can be attributed to inhibition of PIN-mediated export activity.

Whereas previous auxin transport studies have used externally applied NPA by necessity, the oocyte system offers the opportunity to introduce NPA internally or externally, and as this has never been tested, we investigated this. In comparison to internally injected NPA_{in}, adding 10 μM NPA to external medium (NPA_{out}) of pH 7.5 at the start of the assay was ineffective in inhibiting PIN-mediated ^{3}H-IAA export (Fig. 1*A*, NPA_{out}). However, inhibition, was enhanced by either longer preincubation with 10 μM NPA_{out} at pH 7.5 or by changing to a plant-type medium pH of 5.5 (Fig. 1*B*). The more potent immediate effect of NPA_{out} at pH 5.5 and the delayed lesser effect at pH 7.5 suggest that NPA, a weak organic acid, diffuses into oocytes in the uncharged protonated state, with this species being more abundant at the lower pH of 5.5. This is consistent with previous suggestions of passive and pH-dependent uptake into maize coleoptiles (9). More importantly, we show that NPA has to enter cells and bind to an intracellular site to inhibit PIN-mediated ^{3}H-IAA export.

PIN activity in oocytes is kinase-dependent. As the requirement is for active phosphorylation rather than kinase presence per se (32), it was necessary to check if kinase activity was being affected by NPA. PID phosphorylation activity has been reported as NPA-insensitive (25), and here, using in vitro assays, we found that NPA perturbed neither autophosphorylation nor phosphorylation of PIN1 or PIN3 hydrophilic loops by D6PK (Fig. 1*D*). Taken together, as NPA affects neither kinase nor general oocyte transport competence nor background leakage, we conclude that NPA may be targeting PINs themselves at an intracellular site to inhibit PIN-mediated auxin efflux in oocytes.

NPA Binds to Plant Membranes Enriched in NPA-Sensitive PINs. These results prompted us to see if NPA could indeed bind to PINs. Radioligand-binding assays were used to initially establish and characterize high-affinity ^{3}H-NPA binding to plant microsomal membranes (7–10), followed by later reports linking microsomal ^{3}H-NPA–binding profiles to the presence or absence (in mutant lines) of suspected target proteins such as ABCB1/19, TWD1, actin, PID, or BIG/TIR3 (13, 14, 17, 20, 34). Microsomes from *pin1* or *pin2* mutants have been used to argue for the lack of NPA binding by PINs (17, 20), although such interpretation may be unwarranted as single mutants are not devoid of other PIN members. As there are no reports using PIN-enriched samples, we tested this using transient overexpression of *At*PINs in *Nicotiana benthamiana*. To remove nonexpressing cells, we isolated the lower epidermis of infiltrated leaves and used this pure population of transfected cells to prepare membranes highly enriched for the heterologously expressed *At*PINs (*SI Appendix*, Fig. S2*A*). This enabled us to develop a microscale binding assay using minimal amounts of membranes, such that any endogenous NPA binding was at undetectable levels. We also minimized reaction volumes to <10 μL, allowing us to monitor not just binding to membrane pellets but also the corresponding depletions from the supernatant (SN) (*SI Appendix*, Fig. S2*D*). The latter was a more reliable measure as bound ^{3}H-NPA started to dissociate from membranes during washing of pellets. Such rapid dissociation has been reported (7, 8, 10) and agrees with reversible NPA inhibition of PAT in planta (7).

Using competition by excess unlabeled NPA to define specific/saturable binding (8), we found that ^{3}H-NPA bound to membranes expressing *A. thaliana* PIN1, PIN2, PIN3, or PIN6 but not to membranes from mock controls (Fig. 2*A*). Addition of excess IAA or another aromatic acid (benzoic acid [BA]) did not compete with ^{3}H-NPA, showing that the observed binding was specific for NPA and reconfirming that IAA and NPA bind at different sites (7–9). Adding ATP did not hinder binding of ^{3}H-NPA, revealing that NPA cannot mimic the known ability of flavonoids to compete for ATP-binding sites (27, 28). Furthermore, ATP did not enhance ^{3}H-NPA binding in either controls or *At*PIN-expressing membranes, arguing against active ^{3}H-NPA transport into sealed vesicles by ATP-limited transporters (Fig. 2*A*). We could also exclude ^{3}H-NPA transport by PINs, as the added excess IAA would have competed with such transport; this agrees with our oocyte results and confirms that we were detecting binding per se rather than vesicular uptake (8). Binding was reversible, as mentioned above, and saturable by about 100 nM ^{3}H-NPA (*SI Appendix*, Fig. S2*D*), indicating high affinity.

The lack of binding in mock controls (Fig. 2*A*) indicated that overexpressed PINs were required for ^{3}H-NPA binding. We also expressed *Kf*PIN, a functional auxin transporter from the algae *Klebsormidium flaccidum*, but this did not lead to any specific binding of ^{3}H-NPA (*SI Appendix*, Fig. S2 *A* and *B*), which is consistent with *Kf*PIN-mediated auxin export being NPA-insensitive in *Nicotiana* BY2 cells (35). As *Kf*PIN was either exporting auxin by itself or integrating into NPA-insensitive auxin export complexes in the BY2 cells, when interpreted together with the NPA sensitivity of *At*PIN1/3/6-mediated auxin export (1, 33) (Fig. 1 *A* and *C* and *SI Appendix*, Fig. S1*A*), our results show that NPA sensitivity of PINs correlates with their NPA-binding capability, providing additional support for PINs being an NPA-binding component of auxin export.

PIN-Expressing Plant Membranes Are Not Enriched for Other Potential NPA-Binding Proteins. The mock and *Kf*PIN controls suggested that, in the absence of NPA-sensitive PINs, endogenous *N. benthamiana* proteins, membrane lipids or cell walls that were present in the membranes did not detectably contribute to ^{3}H-NPA binding. We were able to exclude any involvement of PIN–cell-wall interactions (5) by using membranes released by enzymatic digestion; these cell-wall–free preparations also bound similar amounts of ^{3}H-NPA (*SI Appendix*, Fig. S2*C*).

To test whether endogenous *N. benthamiana* proteins such as ABCBs or TWD1 were up-regulated in the PIN-overexpressing samples and thus potentially participating or contributing to ^{3}H-NPA binding, we performed quantitative multiplexed mass spectrometry (QMS). Three control and three *At*PIN-expressing samples were labeled with isobaric tags, allowing direct comparison of the relative abundances of endogenous *N. benthamiana* proteins between all six samples. About 3,600 *N. benthamiana* proteins could be quantified (Fig. 2*B*). Based on spectral counts, heterologous *At*PIN1, *At*PIN2, and *At*PIN3 were found to be much more abundant than the only endogenous PIN detected, *Nb*PIN7 (Fig. 2*B* and *SI Appendix*, Table S1). Direct quantitative comparison between *Nb*PIN7 and *At*PIN3 was possible using the relative abundances of shared peptides, revealing that *Nb*PIN7 was at least 20-fold less abundant than *At*PIN3, although this difference is certainly underestimated as interference by technical noise greatly distorts comparison between peptides if they have vastly different relative abundance values, as is the case here (*Materials and Methods*). From immunoblot analysis (*SI Appendix*, Fig. S2*A*), we estimate that *At*PINs were >200-fold more highly expressed in *N. benthamiana* samples when compared to native *At*PIN expression in shoot (36) or to *At*PIN expressed in *N. benthamiana* using native promoter expression (37), providing support that NPA binding could be attributed to an overabundance of *At*PINs.

Global comparison of the relative abundances of 3,687 *N. benthamiana* proteins between controls and PIN samples in QMS revealed no up-regulation of any proteins comparable to the overabundant levels achieved by *At*PINs (Fig. 2 *B* and *C*). Major plasma

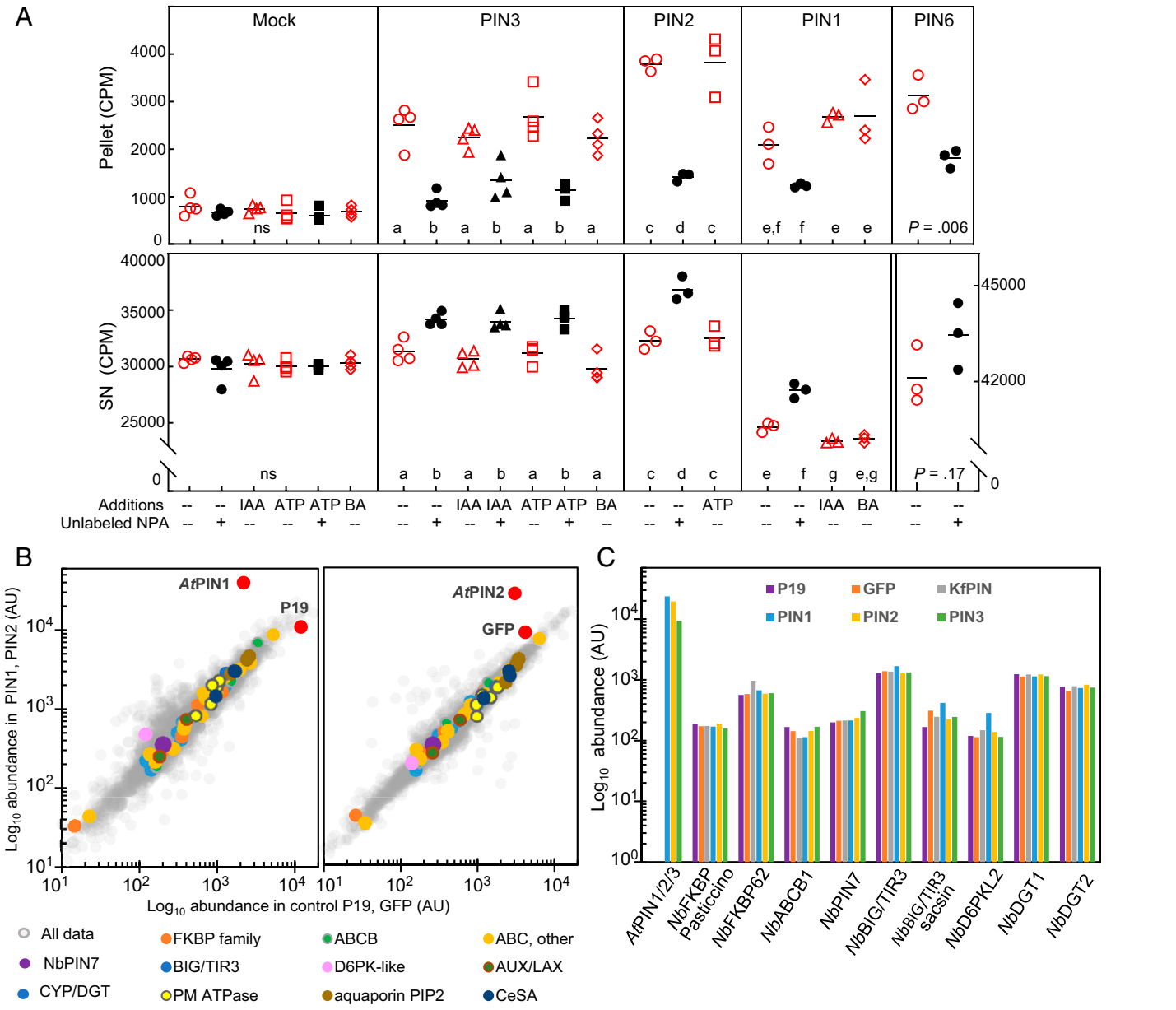

Fig. 2. NPA binds to leaf epidermal membranes overexpressing *At*PINs. (*A*) ^{3}H-NPA binds in a specific/saturable manner to *N. benthamiana* epidermal peel membranes expressing *At*PIN1/2/3/6 but not to membranes from mock controls, with accumulation (open red symbols) in pellet (*Upper*) and depletion from SN (*Lower*) competed by 20 μM unlabeled NPA (filled black symbols). Addition of 20 μM IAA or BA or 3 mM ATP did not compete for binding. Comparisons by *t* test (PIN6, $n = 3$) or ANOVA ($n = 3$ or 4). For pellet: a–b, $P = 0.03$; c–d, $P = 0.001$; e–f, $P = 0.008$. For SN: a–b, $P = 0.004$; c–d, $P = 0.003$; e–f, f–g, $P = 0.001$; e–g, $P = 0.04$. (*B*) Relative abundance values of 3,687 endogenous *N. benthamiana* proteins from QMS analysis (gray cloud; $\log_{10}$ scale; AU, arbitrary units) were compared between controls and PIN-expressing samples (*Left*, P19 vs. PIN1+P19; *Right*, GFP vs. PIN2+GFP). Highlighted *N. benthamiana* proteins are described in the text. Heterologous *At*PIN1/PIN2, GFP, and P19 are shown as red dots; *At*PIN1/PIN2 are plotted against the technical noise in their respective controls (*Materials and Methods*). GFP refers to GFP-KDEL (*SI Appendix*, Fig. S2*F*). (*C*) Relative abundance values of selected *N. benthamiana* proteins from QMS analysis compared across three nonbinding control (P19, GFP, *Kf*PIN) and three overexpressing PIN (*At*PIN1/2/3) samples ($\log_{10}$ scale; AU, arbitrary units). Selected relative abundance values in *B* and *C* are in *SI Appendix*, Table S1.

membrane proteins such as ATPases, aquaporins, and cellulose synthases, as well the auxin transporters AUX/LAX and *Nb*PIN7, were similar between all samples, also indicating equivalent amounts of plasma membranes (Fig. 2 *B* and *C* and *SI Appendix*, Table S1). BIG/TIR3, D6PK-like, and 20 ABC transporters were found, with 6 ABCB-family members including ABCB1 but not ABCB19. *Nb*TWD1/FKBP42 was not detected, which may reflect low abundance in planta, as reported for *At*TWD1 (14, 15). However, five other sequence-related FKBP proteins were detected with *Nb*Pasticcino and *Nb*FKBP62 being most similar to TWD1/FKBP42 (*SI Appendix*, Fig. S2*H*). Nine CYPs were present (*SI Appendix*, Fig. S2*I*), including two orthologs of tomato DGT, annotated here as *Nb*DGT1 and *Nb*DGT2. As *Nb*DGT1/2 are more closely related to tomato DGT (95 to 96% identity) than *A. thaliana* orthologs (*At*ROC1/CYP1; 81% identity to tomato DGT), they may be potential PIN interactors (21). *N. benthamiana* has putative orthologs of *At*APM1 (*SI Appendix*, Fig. S2*I*), but none was detected in the QMS.

For all these endogenous proteins and identified potential NPA-binding or PIN-interacting proteins, we found no up-regulation

suggestive of a stoichiometric complex with overexpressed *At*PINs (Fig. 2 *B* and *C* and *SI Appendix*, Table S1). We cannot rule out that transient chaperone interactions were required to confer NPA-binding ability, or that complexes between overexpressed PINs and other unchanging abundant proteins may have occurred. However, as these along with *Nb*PIN7 and *NbABCB1* remained unchanged and showed no detectable binding in any controls (Fig. 2*A* and *SI Appendix*, Fig. S2 *B–D*), we conclude that, if present, any endogenous interactors did not contribute to the observed ^{3}H-NPA binding and/or that PINs were the necessary NPA-binding component of any such complexes. The lack of detectable binding by *Nb*ABCB1 or *Nb*PIN7 can be attributed to the minimal amounts of material used and low endogenous abundance compared to the highly overexpressed *At*PINs.

As a precise NPA-binding pocket in *At*TWD1 has been identified by NMR analysis (albeit using an unusually high concentration of 3.1 mM NPA due to methodological constraints) (17), we further checked if the other *N. benthamiana* FKBPs found in QMS could be expected to bind NPA. Sequence alignment with *At*TWD1 revealed similarity in only one of the four clusters involved in binding (*SI Appendix*, Fig. S2 *G* and *H*), implying that these *N. benthamiana* FKBPs are unlikely to bind NPA, particularly at the low concentrations (<0.1 μM) of ^{3}H-NPA used compared to the reported K_d of ∼100 μM for *At*TWD1 (17). We also noted that K79 in the second cluster, identified as the most critical residue for NPA binding (17), is not conserved in *Nb*FKBP42, but is instead E79 (*SI Appendix*, Fig. S2*G*). We found that in other plant species, K79 frequently varies as E79/Q79/A79 within an otherwise conserved region of FKBP42 (*SI Appendix*, Fig. S2*K*). As mutating K79 to L79 abolished NPA binding in *At*TWD1 and conferred NPA insensitivity in vivo (17), it would thus be interesting to see if E79/Q79/A79 variants can bind NPA, particularly A79 which resembles the nonbinding L79 mutation.

Overall, our QMS and sequence analysis did not reveal any endogenous proteins that could potentially account for the observed NPA binding, leaving the enriched heterologous *At*PINs as the most plausible NPA-binding component in this experimental setup.

NPA Binds to Heterologous PIN-Enriched Membranes and Is Independent of Phosphorylation. To further confirm PINs as the NPA-binding component, we repeated the binding assays using *At*PINs expressed in nonplant hosts (*SI Appendix*, Fig. S3 *C–E*). Membranes from oocytes (PIN1) as well as yeast (PIN6:GFP) both bound ^{3}H-NPA in a specific/saturable manner whereas nonexpressing controls did not, with excess BA in all samples not competing for binding (Fig. 3 *A* and *B*). This shows that plant-derived components are not required, agreeing with our QMS results that endogenous *N. benthamiana* proteins were not contributing to NPA binding. Furthermore, as PIN-expressing oocyte membranes bound NPA in this in vitro setting, this suggests that the in vivo transport inhibition observed was not due to NPA perturbing transient chaperone or trafficking events in oocytes, as these are not expected to occur in isolated membranes.

In oocyte membranes, NPA binding was independent of PIN1 hydrophilic loop phosphorylation as similar binding occurred with or without D6PK phosphorylation of PIN1 (Fig. 3*A*), which can be detected in PIN1 immunoblots by slower migration and a phosphorylation smear (32, 37) (Fig. 3*C*) and which was stable throughout the binding assay. D6PK itself did not participate in ^{3}H-NPA binding, as it partitioned into the SN and was absent from the membrane fraction used for binding assays (Fig. 3*D*). The *N. benthamiana* ^{3}H-NPA binding results also gave no indication of phosphorylation requirements in that we did not attempt to preserve phosphatase-sensitive phosphorylation during membrane extraction and thus PIN1 and PIN3 in the *N. benthamiana* membranes were no longer phosphorylated (no smear detected in immunoblots) whereas PIN2 had some residual smear (*SI Appendix*, Fig. S2*A*), yet all were able to bind NPA (Fig. 2*A*). We further checked the effect of NPA on in vivo steady-state phosphorylation of PIN in plant cells, where multiple kinases and phosphatases would contribute (37). Using *35S:PIN1* to avoid complications from transcriptional responses, we found no reduction in the PIN1 phosphorylation smear, noting also that PIN stability was unaffected by NPA (Fig. 3*E*). Thus, NPA does not impinge on global PIN phosphorylation status in vivo, agreeing with our in vitro data (Fig. 1*D*), and neither phosphorylation nor

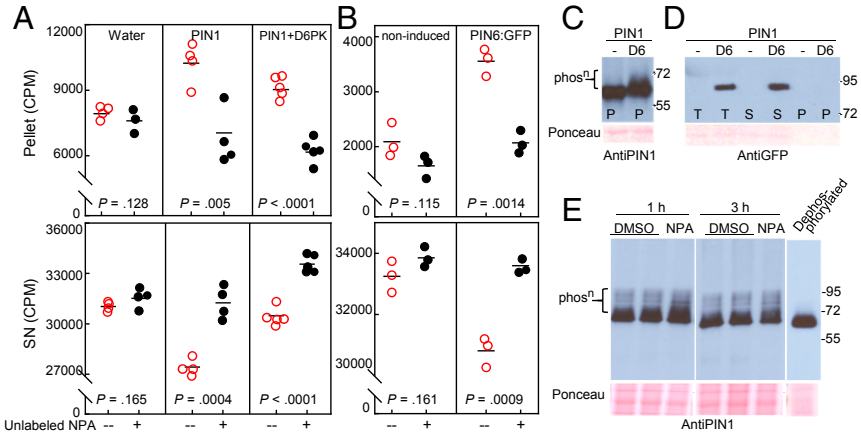

Fig. 3. NPA binds to oocyte and yeast membranes expressing PINs. (*A*) ^{3}H-NPA binds in a specific/saturable manner to membranes from oocytes expressing PIN1 or PIN1+YFP:D6PK but not to membranes from control oocytes (injected with water instead of RNA), with an increase in pellet (red symbols, *Upper*) and depletion in SN (red symbols, *Lower*) compared to samples with 30 μM unlabeled NPA (black symbols) (*t* test, $n = 4$ to 5). All samples contained 30 μM BA. (*B*) ^{3}H-NPA binds in a specific/saturable manner to membranes from yeast expressing PIN6:GFP but not to noninduced control membranes with an increase in pellet (red symbols, *Upper*) and depletion in SN (red symbols, *Lower*) compared to samples with 30 μM unlabeled NPA (black symbols) (*t* test, $n = 3$). All samples contained 15 μM BA. (*C*) Anti-PIN1 immunoblots using membranes from PIN1 + YFP:D6PK (D6) oocytes detect PIN1 traveling as a slower migrating species with a smear, indicative of YFP:D6PK-mediated phosphorylation, which is not seen when PIN1 is expressed alone. (*D*) YFP:D6PK (D6) partitioned into the soluble SN fraction (S) and was not detectable in the oocyte membrane pellet fraction (P) used for binding assays (T, total extract; antiGFP immunoblot). (*E*) In *35S:PIN1* suspension culture cells, 10 μM NPA treatment (1 to 3 h) did not reduce the endogenous PIN1 phosphorylation smear (antiPIN1 immunoblot). Dephosphorylated PIN1 is shown for comparison.

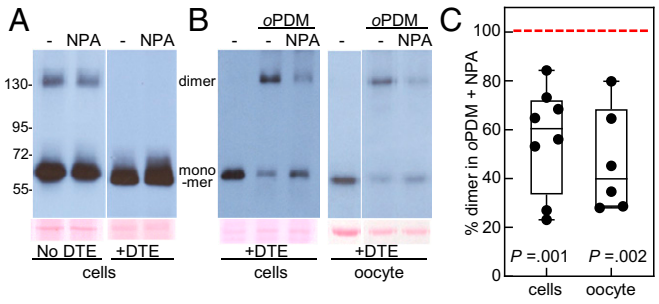

Fig. 4. NPA inhibits *o*PDM cross-linking of PIN1 into dimers.(*A*) Endogenous PIN1 dimers seen in nonreducing SDS/PAGE (No DTE) are unaffected by in vivo NPA treatment of suspension cells (10 μM, 2 h; antiPIN1 immunoblot). (*B*) In membranes from suspension cells or oocytes, PIN1 is cross-linked into DTE-resistant dimers by *o*PDM in vitro, and this is inhibited by NPA (antiPIN1 immunoblot). (*C*) Monomers and cross-linked PIN1 dimers from *o*PDM treatments (± NPA) were quantified from immunoblots and dimer:monomer ratios were calculated. The ratio in *o*PDM+NPA was compared to *o*PDM+DMSO by a one-sample *t* test with the latter used as the test value of 100% as indicated by the dashed red line. NPA reduced the amount of *o*PDM-linked PIN1 dimers in both suspension cells ($n = 8$, 95% CI [26, 62]) and oocytes ($n = 6$, 95% CI [31, 75]).

kinase appear to be required or inhibitory for NPA association with PINs.

In summary, we found that ^{3}H-NPA binding to *N. benthamiana*, oocytes, and yeast membranes correlates with the overexpression of *At*PINs, independent of host, phosphorylation status, or other plant proteins or cell-wall components, collectively supporting a direct association with PINs or a major role for PINs in enhancing NPA binding to PIN-enriched membranes.

NPA Interferes with a PIN Dimer Interface. As we saw NPA binding as well as NPA inhibition of PIN activity in oocytes, we sought a mechanism that might explain or connect these two observations. We found that PINs form disulfide-dependent dimers that are visible in nonreducing sodium dodecyl sulfate/polyacrylamide gel electrophoresis (SDS/PAGE) and which are not affected by NPA (Fig. 4*A*). However, we then treated plant or oocyte membranes with *ortho*-phenylenedimaleimide (*o*PDM), a bifunctional reagent that can covalently cross-link two vicinal free cysteines (Cys). This led to *o*PDM-linked PIN dimers now resistant to reducing agents such as dithioerythritol (DTE) (Fig. 4*B*), and we found that less cross-linking occurred when NPA was present (Fig. 4 *B* and *C*). This effect was seen with both PIN1 and PIN2 from cultured plant cells as well as with PIN1 from oocytes (Fig. 4 *B* and *C* and *SI Appendix*, Fig. S4*A*), indicating a property inherent of PINs and independent of the host membrane. The cross-linking of other proteins in the same sample was not affected by NPA (*SI Appendix*, Fig. S4 *C* and *D*), and we further confirmed that NPA did not affect the chemical reactivity of *o*PDM or Cys (*SI Appendix*, Fig. S4*B*). We also checked other compounds and found that neither auxins (IAA or 1-naphthylacetic acid [NAA]) nor the alternative PAT inhibitor 2,3,5-triiodobenzoic acid (TIBA) could inhibit cross-linking of PINs by *o*PDM (*SI Appendix*, Fig. S4 *D* and *E*).

These data support an inhibitory effect on cross-linking of PINs that was unique for NPA and suggestive of an interaction between NPA and PIN. Possible explanations are that NPA binds near a Cys to sterically hinder the reaction with *o*PDM, or elsewhere to cause a conformational change, or that NPA can prise PIN monomers apart beyond the 9-Å maximum cross-linking span of *o*PDM (38). This observation is reminiscent of NPA disrupting TWD1-ABCB1 interaction (14), although NPA is proposed to bind to soluble domains in TWD1 or ABCB1 (14, 17, 20), whereas all Cys in PIN1/2 are predicted to be in putative transmembrane domains or in short membrane-proximal cytoplasmic loops. Thus, the NPA effect on PINs appears to be different from that of TWD1/ABCB in involving transmembrane domains rather than soluble regions, agreeing with reports describing NPA-binding sites as membrane-integral (10). We note that the predicted cytoplasmic locations for Cys in PIN1/2 are consistent with our oocyte results of an intracellular NPA-binding site.

Since we used intact membranes for both ^{3}H-NPA binding and *o*PDM cross-linking, we cannot rule out that NPA interaction involves the immediate lipid environment of PINs, particularly as PIN activity (Fig. 1) and oligomerization (Fig. 4) are affected and as lipids are known to be important regulators of both in transporters and membrane proteins in general (39, 40). However, as we used three different phyla (plants, animals, fungi) known to have very different membrane lipid composition (39), it seems that PINs themselves are the determining factor in shaping any potential NPA–lipid interaction. Additionally, although ABCBs may stabilize PINs in certain sterol domains in plants and yeast (15), the ability of PINs to function in foreign oocyte membranes is now accepted as evidence that neither ABCB chaperoning nor specialized plant lipid domains are essential for PIN activity (12).

Notwithstanding any lipid involvement, NPA was able to bind to as well as inhibit cross-linking of PINs in oocyte membranes. Thus, a possible explanation for the transport inhibition in oocytes could be an NPA–PIN interaction that leads to conformational or structural perturbations in PINs, providing a potential mechanism for PIN inactivation and inviting consideration of using NPA as a structural or functional activity probe for PINs.

Conclusions

Our data provide an evidential basis to invoke a straightforward mechanistic explanation for NPA inhibition of PINs, in which NPA can bind to PINs independently of other potential NPA-binding proteins. Direct PIN inhibition offers a physiologically relevant model of NPA action and a parsimonious hypothesis to plan and interpret future work, as an alternative to, or combined with, current indirect models. It may also be prudent to reinterpret past work in light of our results to reconsider possible overlooked effects or contributions due to NPA binding by PINs.

The combination of existing models with the one presented here means that NPA could synergistically inhibit both PIN- and ABCB-based major auxin streams. Since it is unlikely to be due to chance that a synthetic compound binds diverse targets (ABCB, PIN, TWD1) in a common auxin export pathway, one way to explain this apparent coincidence is the concept that NPA mimics an endogenous counterpart which has evolved to do precisely so. Our results provide hints as to how NPA or an endogenous inhibitor may interact with PINs, namely an intracellular allosteric site distinct from IAA substrate-binding sites, possibly involving membrane-proximal conserved Cys residues and an interface between monomers. Any involvement of the PIN hydrophilic loop is restricted to the ∼100 residues shared between canonical PIN1/2/3 and the shorter loop of PIN6. Furthermore, binding is independent of the many phosphorylation sites contained therein and does not require loop kinases. Further investigations into these and other aspects of NPA–PIN interactions are warranted with the collateral benefit of gaining much needed structural and mechanistic insights into PINs.

Materials and Methods

Oocyte Transport. Oocytes were injected with ^{3}H-IAA or ^{3}H-NPA (American Radiolabeled Chemicals) (32). NPA was coinjected with ^{3}H-IAA (1 or 10 μM final internal concentration; NPA_{in}) or added into the medium (10 μM final external; NPA_{out}) at 0, 10, or 150 min before injecting ^{3}H-IAA. Results are presented as "relative IAA content" (^{3}H-IAA cpm in oocytes at 30 vs. 0 min) or as transport rates from linear regression of a cpm vs. time plot, translated to fmol based on the specific activity of ^{3}H-IAA. External medium was Barth's solution (32) with 10 mM Hepes, pH 7.5 or 5.5. For AUX1/^{3}H-IAA (41) and CAT6/^{14}C-leucine (ARC) (42) assays, oocytes were injected with 10 μM NPA_{in}, and results are presented as cpm in oocytes at the end of assays.

Phosphorylation and Dimers. In vitro [γ-^{32}P]-*ATP* phosphorylation assays were performed with ±10 μM NPA (32). For global phosphorylation or endogenous dimer analysis, *35S:PIN1* suspension cells were treated with 10 μM NPA or dimethylsulfoxide (DMSO) (1 to 4 h in 0.5x Murashige–Skoog medium [MSM]), and membranes were extracted (36, 37).

***N. benthamiana* Membranes.** *At*PIN1/2/3/6 or *Kf*PIN (in pMDC7 or pK7WG2D) were agroinfiltrated together with P19 (43) into *N. benthamiana* leaves. Mock controls received empty vectors and/or P19. Leaves with pMDC7 were induced (24 h, 2 μM β-estradiol/0.2x MSM). The lower epidermis was peeled off, and membranes were extracted by homogenization (36) or released by digestion (1 h, 4 °C, 0.07% cellulase/0.03% macerozyme in 50 mM Tris–HCl, pH 7.4/5 mM ethylenediaminetetraacetic acid [EDTA]/0.05% casein/2% glycerol [EB] with 1 mM phenylmethylsulfonyl fluoride [PMSF]/1 μg/mL aprotinin/leupeptin/pepstatin/E64 [PI]). Membranes were collected (45,000 x *g*, 30 min, 4 °C), washed (20 mM Tris–HCl, pH 8/5 mM EDTA [TE]), and resuspended in EB + PI.

Yeast Membranes. *At*PIN6 in pDDGFP_LEU2D was transformed into *Saccharomyces cerevisiae* BJ5460. Cultures started in LEU-dropout medium +2% lactate (from OD 0.05 to 0.6) were induced with 2% galactose (20 h, 30 °C) (*SI Appendix*, Fig. S3*D*). Yeast were spheroplasted using Zymolase 20T (Roth), disrupted in TE + PI, and twice spun through 5% glycerol/TE/1 mM PMSF onto a 0.1-mL 50% sucrose cushion (45,000 x *g*, 30 min, 4 °C). Membrane pellets were resuspended in 5% glycerol/TE/1 mM PMSF.

Oocyte Membranes. Oocytes were homogenized (100 mM Tris–HCl, pH 7.5/10 mM EDTA/5 mM EGTA/0.1% casein/10% glycerol/50 mM NaF/20 mM β-glycerol PO_4/10 mM $NaMO_4$/Phosstop/PI), and a crude pellet was collected (45,000 x *g*, 30 min, 4 °C). Yolk proteins (vitellogenins) were removed from this pellet by successive washing with 100 mM $MgCl_2$, 1 M NaCl, and TE (modified from ref. 44) (*SI Appendix*, Fig. S3*A*) and resuspended in EB + PI. Residual vitellogenin was similar in all samples (*SI Appendix*, Fig. S3*B*). Control water-injected and RNA-injected oocytes were prepared from the same batches.

Radioligand Binding Assay. We modified previous assays (7–10) into a microscale assay (<10 μL). Each reaction contained membranes (1 to 3 μL pellet volume) from 15 to 30 mg *N. benthamiana* peel, 12 OD units yeast or two oocytes, in all cases ~100 to 300x the amounts required to obtain a very strong signal in immunoblot analysis of PIN expression levels (*SI Appendix*, Figs. S2*A* and S3 *C* and *E*). For each series, equal aliquots of membranes were pelleted (21,000 x *g*, 30 min, 4 °C) and washed with 20 mM $MgCl_2$, and all traces of supernatant removed. The pellet was carefully resuspended in an exact volume (3 to 6 μL) of binding buffer (RB: 5% glycerol/0.1 mM $MgSO_4$/5 mM KCl and 50 mM $KHPO_4$/$NaHPO_4$, pH 6.5 or 7.5) containing ^{3}H-NPA (~0.05 μCi, 60 Ci/mmol) and 1-μL additions (unlabeled NPA, BA, or IAA (20- to 30-μM final concentrations) or ATP (3-mM final concentration, pH adjusted to 7.4 with two molar equivalents of Tris base) or solvent (DMSO or pH 7.4 Tris–HCl). When ATP was used, 5 mM $MgCl_2$ was included in the whole series. All yeast (15 μM) and oocyte (30 μM) samples contained BA. After 2 to 6 h, samples were spun (21,000 x *g*, 15 min, 4 °C), and a precise volume of SN was removed. Pellets were counted directly (as in refs. 7–9), or washed by quickly transferring to GF/F Whatman filters (as in ref. 10) using 10 μL RB and rapidly washing with 3x 0.7 mL RB/0.1 μM BA in a vacuum manifold. Radioactivity in pellets, filters, and SN was measured by liquid scintillation counting, and results are reported as cpm (61% counting efficiency). A typical reaction contained a 1.5-μL membrane pellet resuspended in 6 μL, from which 5 or 6 μL SN was subsequently removed for washed or unwashed pellets, respectively (*SI Appendix*, Fig. S2*D*). Accurate pipetting was essential for this microscale assay; we used low-binding extrafine-tipped pipette tips (10 μL extralong Surphob Tips, Biozym) and an Eppendorf 10-μL pipette with a metal-tip cone and volume lock. ^{3}H-NPA was used within 2.5 y of purchase.

Cross-linking. Membranes from cells or oocytes were pretreated with 20 to 50 μM NPA, TIBA, NAA, IAA, or DMSO (30 to 60 min; 0.2 M $NaHPO_4$ pH 7.5/10% glycerol or RB), cross-linked (5 to 60 min, 0.2 to 0.5 mM *o*PDM [Sigma] or DMSO) and quenched (5 mM *N*-ethylmaleimide or 20 mM DTE followed by 60 mM *N*-ethylmaleimide). NPA did not affect the chemical reactivity or stability of *o*PDM or Cys, tested using Ellman's reagent/DTNB ($Abs_{412\ nm}$) (*SI Appendix*, Fig. S4*B*).

Immunoblotting. Membrane fractions were prepared as above or as in ref. 36. Membranes from <0.1 mg *N. benthamiana* peel, 1/50th oocyte, or 0.1 OD units yeast were blotted (36, 37) and probed with antiPIN1 or antiPIN2 (36), antiPIN3 (45), anti*Kf*PIN (35), antiGFP (Roche) or rabbit antiPIN6 raised against residues 167 to 405 of *At*PIN6. Molecular weight markers and Ponceau-stained blots are shown next to immunoblots. Bands were quantified from images captured using ImageLab/ChemiDocXRS (Biorad).

QMS. Equal amounts of *N. benthamiana* membranes from three controls (P19, GFP-KDEL, *Kf*PIN) and three *At*PIN-expressing samples (PIN1, PIN2+GFP-KDEL, PIN3; all six samples contained P19) were sequentially solubilized with 2% dodecylmaltoside, 0.4% SDS, and 0.5% sodium deoxycholate (*SI Appendix*, Fig. S2 *E* and *F*), precipitated with $CHCl_3$/MeOH, solubilized with a graded ethanol series, labeled using isobaric TMTsixplex as per the manufacturer's instructions (Thermo Fisher Scientific) and combined for QMS (46). We used the *N. benthamiana* NbDE proteome database (47). Sequences were analyzed in MEGA-X using multiple alignment by ClustalW or MUSCLE with manual curation. For heterologous proteins (*At*PIN, GFP-KDEL), the apparent relative abundance values in the other nonexpressing samples are technical noise from the overtly overexpressing sample(s) due to precursor ion impurity and coisolation. We confirmed this using an alternate SPS3 data-acquisition regime, where noise values for PIN1 were reduced from 5–11% (*SI Appendix*, Table S1) to 0–0.6% in SPS3 and for PIN2 from 9–17% to 0.6–1.5%. Similarly, direct quantitative comparison using shared peptides between *At*PIN and *Nb*PIN7 was unreliable as the extreme differences in relative abundances caused technical noise in the nonexpressing samples. Fig. 2*C* uses relative abundance values normalized using global average relative abundance from 3,687 *N. benthamiana* proteins detected in each sample (*SI Appendix*, Table S1).

Statistics. Data were analyzed in Microsoft Excel 2016, IBM SPSS Statistics v24, or GraphPad Prism8. Unpaired *t* tests (two-tailed *P* values) were used, except for Fig. 3*C* (one-sample *t* test). One-way ANOVA was used unless otherwise stated and was not significant (ns) if $P > 0.05$. Post-hoc analysis was by Holm–Sidak, Dunn, or Tukey's tests; lowercase letters indicate homogeneous subsets. For ^{3}H-NPA–binding data, bars show means.

Data Availability. All study data are included in the article and supporting information.

ACKNOWLEDGMENTS. This work was supported by Austrian Science Fund Grant FWF P21533-B20 (to L.A.); German Research Foundation Grant DFG HA3468/6-1 (to U.Z.H.); and European Research Council Grant 742985 (to J.F.). We thank Herta Steinkellner and Alexandra Castilho for *N. benthamiana* plants, Fabian Nagelreiter for statistical advice, Lanassa Bassukas for help with [γ-^{32}P]-*ATP* assays, and Josef Penninger for providing access to mass spectrometry instruments at the Vienna BioCenter Core Facilities. We thank PNAS reviewers for the many comments and suggestions that helped to improve this manuscript.

1. J. Petrášek *et al.*, PIN proteins perform a rate-limiting function in cellular auxin efflux. *Science* **312**, 914–918 (2006).
2. L. Gälweiler *et al.*, Regulation of polar auxin transport by AtPIN1 in Arabidopsis vascular tissue. *Science* **282**, 2226–2230 (1998).
3. J. Wiśniewska *et al.*, Polar PIN localization directs auxin flow in plants. *Science* **312**, 883 (2006).
4. E. Benková *et al.*, Local, efflux-dependent auxin gradients as a common module for plant organ formation. *Cell* **115**, 591–602 (2003).
5. M. Adamowski, J. Friml, PIN-dependent auxin transport: Action, regulation, and evolution. *Plant Cell* **27**, 20–32 (2015).
6. W. Teale, K. Palme, Naphthylphthalamic acid and the mechanism of polar auxin transport. *J. Exp. Bot.* **69**, 303–312 (2018).
7. K. S. Thomson, R. Hertel, S. Müller, J. E. Tavares, 1-N-naphthylphthalamic acid and 2,3,5-triiodobenzoic acid : In-vitro binding to particulate cell fractions and action on auxin transport in corn coleoptiles. *Planta* **109**, 337–352 (1973).
8. M. R. Sussman, G. Gardner, Solubilization of the receptor for N-1-naphthylphthalamic acid. *Plant Physiol.* **66**, 1074–1078 (1980).
9. M. R. Sussman, M. H. M. Goldsmith, The action of specific inhibitors of auxin transport on uptake of auxin and binding of N-1-naphthylphthalamic acid to a membrane site in maize coleoptiles. *Planta* **152**, 13–18 (1981).
10. P. Bernasconi, B. C. Patel, J. D. Reagan, M. V. Subramanian, The N-1-Naphthylphthalamic acid-binding protein is an integral membrane protein. *Plant Physiol.* **111**, 427–432 (1996).
11. K. Okada, J. Ueda, M. K. Komaki, C. J. Bell, Y. Shimura, Requirement of the auxin polar transport system in early stages of Arabidopsis floral bud formation. *Plant Cell* **3**, 677–684 (1991).
12. M. Geisler, B. Aryal, M. di Donato, P. Hao, A critical view on ABC transporters and their interacting partners in auxin transport. *Plant Cell Physiol.* **58**, 1601–1614 (2017).
13. B. Noh, A. S. Murphy, E. P. Spalding, Multidrug resistance-like genes of Arabidopsis required for auxin transport and auxin-mediated development. *Plant Cell* **13**, 2441–2454 (2001).

14. A. Bailly *et al*., Modulation of P-glycoproteins by auxin transport inhibitors is mediated by interaction with immunophilins. *J. Biol. Chem.* **283**, 21817–21826 (2008).
15. B. Titapiwatanakun *et al*., ABCB19/PGP19 stabilises PIN1 in membrane microdomains in Arabidopsis. *Plant J.* **57**, 27–44 (2009).
16. G. Wu, M. S. Otegui, E. P. Spalding, The ER-localized TWD1 immunophilin is necessary for localization of multidrug resistance-like proteins required for polar auxin transport in Arabidopsis roots. *Plant Cell* **22**, 3295–3304 (2010).
17. J. Zhu *et al*., TWISTED DWARF1 mediates the action of auxin transport inhibitors on actin cytoskeleton dynamics. *Plant Cell* **28**, 930–948 (2016).
18. J. J. Blakeslee *et al*., Interactions among PIN-FORMED and P-glycoprotein auxin transporters in Arabidopsis. *Plant Cell* **19**, 131–147 (2007).
19. J. Mravec *et al*., Interaction of PIN and PGP transport mechanisms in auxin distribution-dependent development. *Development* **135**, 3345–3354 (2008).
20. J.-Y. Kim *et al*., Identification of an ABCB/P-glycoprotein-specific inhibitor of auxin transport by chemical genomics. *J. Biol. Chem.* **285**, 23309–23317 (2010).
21. M. Geisler, A. Bailly, M. Ivanchenko, Master and servant: Regulation of auxin transporters by FKBPs and cyclophilins. *Plant Sci.* **245**, 1–10 (2016).
22. T. Paciorek *et al*., Auxin inhibits endocytosis and promotes its own efflux from cells. *Nature* **435**, 1251–1256 (2005).
23. J. Petrásek *et al*., Do phytotropins inhibit auxin efflux by impairing vesicle traffic? *Plant Physiol.* **131**, 254–263 (2003).
24. P. Dhonukshe *et al*., Auxin transport inhibitors impair vesicle motility and actin cytoskeleton dynamics in diverse eukaryotes. *Proc. Natl. Acad. Sci. U.S.A.* **105**, 4489–4494 (2008).
25. S. Henrichs *et al*., Regulation of ABCB1/PGP1-catalysed auxin transport by linker phosphorylation. *EMBO J.* **31**, 2965–2980 (2012).
26. D. E. Brown *et al*., Flavonoids act as negative regulators of auxin transport in vivo in Arabidopsis. *Plant Physiol.* **126**, 524–535 (2001).
27. G. Conseil *et al*., Flavonoids: A class of modulators with bifunctional interactions at vicinal ATP- and steroid-binding sites on mouse P-glycoprotein. *Proc. Natl. Acad. Sci. U.S.A.* **95**, 9831–9836 (1998).
28. C. Gu *et al*., Inhibition of inositol polyphosphate kinases by quercetin and related flavonoids: A structure-activity analysis. *J. Med. Chem.* **62**, 1443–1454 (2019).
29. H. Fujita, K. Syōno, PIS1, a negative regulator of the action of auxin transport inhibitors in Arabidopsis thaliana. *Plant J.* **12**, 583–595 (1997).
30. N. Geldner, J. Friml, Y.-D. Stierhof, G. Jürgens, K. Palme, Auxin transport inhibitors block PIN1 cycling and vesicle trafficking. *Nature* **413**, 425–428 (2001).
31. W. A. Peer *et al*., Mutation of the membrane-associated M1 protease APM1 results in distinct embryonic and seedling developmental defects in Arabidopsis. *Plant Cell* **21**, 1693–1721 (2009).
32. M. Zourelidou *et al*, Auxin efflux by PIN-FORMED proteins is activated by two different protein kinases, D6 PROTEIN KINASE and PINOID. *Elife* **3**, e02860 (2014).
33. S. Simon *et al*., PIN6 auxin transporter at endoplasmic reticulum and plasma membrane mediates auxin homeostasis and organogenesis in Arabidopsis. *New Phytol.* **211**, 65–74 (2016).
34. M. Ruegger *et al*., Reduced naphthylphthalamic acid binding in the *tir3* mutant of Arabidopsis is associated with a reduction in polar auxin transport and diverse morphological defects. *Plant Cell* **9**, 745–757 (1997).
35. R. Skokan *et al*., PIN-driven auxin transport emerged early in streptophyte evolution. *Nat. Plants* **5**, 1114–1119 (2019).
36. L. Abas, C. Luschnig, Maximum yields of microsomal-type membranes from small amounts of plant material without requiring ultracentrifugation. *Anal. Biochem.* **401**, 217–227 (2010).
37. S. Tan *et al*., Salicylic acid targets protein phosphatase 2A to attenuate growth in plants. *Curr. Biol.* **30**, 381–395.e8 (2020).
38. N. S. Green, E. Reisler, K. N. Houk, Quantitative evaluation of the lengths of homobifunctional protein cross-linking reagents used as molecular rulers. *Protein Sci.* **10**, 1293–1304 (2001).
39. M. Opekarová, W. Tanner, Specific lipid requirements of membrane proteins: A putative bottleneck in heterologous expression. *Biochim. Biophys. Acta* **1610**, 11–22 (2003).
40. K. Gupta *et al*., The role of interfacial lipids in stabilizing membrane protein oligomers. *Nature* **541**, 421–424 (2017).
41. Y. Yang, U. Z. Hammes, C. G. Taylor, D. P. Schachtman, E. Nielsen, High-affinity auxin transport by the AUX1 influx carrier protein. *Curr. Biol.* **16**, 1123–1127 (2006).
42. U. Z. Hammes, E. Nielsen, L. A. Honaas, C. G. Taylor, D. P. Schachtman, AtCAT6, a sink-tissue-localized transporter for essential amino acids in Arabidopsis. *Plant J.* **48**, 414–426 (2006).
43. F. Garabagi, E. Gilbert, A. Loos, M. D. McLean, J. C. Hall, Utility of the P19 suppressor of gene-silencing protein for production of therapeutic antibodies in *Nicotiana* expression hosts. *Plant Biotechnol. J.* **10**, 1118–1128 (2012).
44. M. J. Bergeron *et al*., Frog oocytes to unveil the structure and supramolecular organization of human transport proteins. *PLoS One* **6**, e21901 (2011).
45. M. M. Marquès-Bueno, J. Moreno-Romero, L. Abas, R. De Michele, M. C. Martínez, A dominant negative mutant of protein kinase CK2 exhibits altered auxin responses in Arabidopsis. *Plant J.* **67**, 169–180 (2011).
46. L. Zhang, J. E. Elias, "Relative protein quantification using tandem mass tag mass spectrometry" in *Proteomics. Methods in Molecular Biology*, L. Comai, J. Katz, P. Mallick, Eds. (Humana Press, New York, 2017), vol. 1550, pp. 185–198.
47. J. Kourelis *et al*., A homology-guided, genome-based proteome for improved proteomics in the alloploid *Nicotiana benthamiana*. *BMC Genomics* **20**, 722 (2019).